

Linear Influence of Weak Magnetic Field on Critical Temperature T_c of HTS Material $YBa_2Cu_3O_{7-\delta}$

Yisi Liu¹, Feifei Xiao¹, Mo Cheng¹.

Instructor: Professor Wang Kai

School of Physics and Astronomy, Sun Yat-sen University, ZhuHai, China.

Abstract

We employed BCS theory to analyze the behavior of the critical temperature of $YBa_2Cu_3O_{7-\delta}$ under a weak magnetic field environment. Our theoretical framework and experimental results demonstrate that a weak magnetic field ($\leq 1T$) may exhibit a linear effect on the critical temperature. This suggests that BCS theory can provide an explanation for certain phenomena observed in specific high-temperature superconducting materials.

Keywords: $YBa_2Cu_3O_{7-\delta}$, BCS Theory, Critical Temperature, Weak Magnetic Field.

1 Introduction

High-temperature superconductors (HTS) have garnered significant attention since their discovery in 1986 [1]. They surpassed the temperature limitations of traditional superconductors, indicating the existence of a novel mechanism in HTS materials. HTS has found widespread applications in various areas, such as the Maglev system in Shanghai. Therefore, comprehending the mechanisms underlying HTS and discovering more practical HTS materials holds considerable importance and necessity.

The critical temperature denotes the temperature at which a material transitions from a normal state to a superconducting state. Superconductivity manifests only when the environmental temperature is below the critical temperature. Unlike low-temperature superconductors, HTS typically possesses critical temperatures above 40K, making them more attainable. The critical temperature of a superconductor can be influenced by environmental magnetic fields [2], with numerous studies examining the effects of high magnetic fields [2, 8, 9, 10]. However, the influence of weak magnetic fields remains inadequately explored. In this study, we focus on the material $YBa_2Cu_3O_{7-\delta}$ to learn its influence.

While BCS theory is a classical approach employed to comprehend the electromagnetic and thermal properties of solid-state materials, it does not accurately explain the behavior of HTS [1]. Nonetheless, it can offer insights into their behavior under specific conditions, such as weak magnetic fields. We will delve into the specific details in the subsequent sections.

In our theory and experiment, we make the following assumptions: (i) The alternative electric fields are relatively weak signals compared to the noise, allowing us to neglect the material's impact on the environmental magnetic field. (ii) The susceptibilities of other materials are sufficiently

small to be disregarded. (iii) All assumptions inherent to BCS theory.

2 Theory

2.1 Critical Temperature T_c

In BCS theory[3], the probability of a fermi quasi-particle that it is excited in thermal equilibrium is determined by Fermi function:

$$f(E_k) = \frac{1}{e^{\frac{E_k}{k_B T}} + 1} \quad (1)$$

Where $E_k(\geq \Delta(T)) = (\xi_k^2 + \Delta_k^2)^{1/2}$ is the excitation energy of the fermi quasi-particle. $\xi_k = \epsilon_k - \mu$ is the single-particle energy relative to the Fermi energy and ϵ_k is the eigen energy, $\mu = \mu(T)$ is called the chemical potential. T is the experimental temperature. $k_B = 1.38 \times 10^{-23} J/K$ is the Boltzmann constant.

And Δ_k is determined by

$$\Delta_k = \begin{cases} \Delta(T) & , |\xi_k| < \hbar\omega_c \\ 0 & , |\xi_k| > \hbar\omega_c \end{cases} \quad (2)$$

where $\Delta(T)$ represents the energy gap.

According to Michael Tinkham[3], the critical temperature is determined by

$$\frac{\Delta(0)}{k_B T_c} = b \quad (3)$$

where T_c is the critical temperature of the superconductor. The numerical factor b is an experimental value(which usually falls within the range from 3.0 to 4.5)[3].

Thus, the critical temperature of the superconductor depends on

$$T_c = \frac{\Delta(0)}{bk_B} \quad (4)$$

2.2 Influence of Weak Magnetic Field B

In weak magnetic field environments, the excitation energy of quasi-particle is given by $E_k^{(B)}$, where

$$E_k^{(B)} = E_k - Ng\mu_B B \quad (5)$$

and $\mu_B = 9.27 \times 10^{-24} J/T$ is the Bohr magneton and $g \approx 2$ is the Landé g -factor of the quasi-particle. B denotes the experimental magnetic field. In our experiment, $B \leq 2kG$ is a weak magnetic field (since $\mu_B B \ll k_B T_c$, $T_c \approx 90K$). $N \approx 2 + 2 \times 2 + 1 \times 3 = 9$ corresponds to the approximate number of free electrons in a primitive cell since a phonon is a neutral quasi-particle.

Thus, the critical temperature $T_c^{(B)}$ under weak magnetic field is linearly dependent of B by

$$T_c^{(B)} = T_c - \frac{Ng\mu_B}{bk_B} B \quad (6)$$

The absolute slope k can be accurately determined by

$$k = \frac{Ng\mu_B}{bk_B} \approx \frac{1.21}{b} \in (0.269, 0.403) K/kG \quad (7)$$

3 Experiment

We have discussed the theoretical relationship between the critical temperature T_c and the magnetic field B . Below, we present the theoretical framework and experimental methodology we employed to detect and quantify the critical temperature T_c in our experiment.

3.1 AC Magnetic Susceptibility

According to D. and J.[4], we can use AC magnetic susceptibility to detect T_c

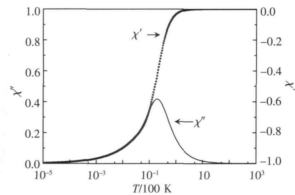


Fig1. The theoretical Curve of AC magnetic susceptibility. χ' is the real part and χ'' is the imaginary part.

The critical temperature T_c is determined by identifying either the peak temperature of the imaginary part of the AC magnetic susceptibility curve or the midpoint temperature of the decreasing part of the real part of the AC magnetic susceptibility curve.

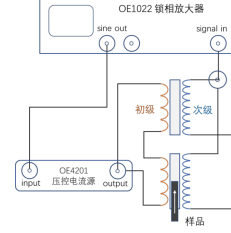


Fig2. The schematic diagram of our experiment

In our experiment, the electrical signal of AC magnetic susceptibility is a weak electromagnetic field signal. Therefore we use lock-in amplifier OE1022 to magnify our signal by so-called *half bridge method*.

AC magnetic susceptibility $\tilde{\chi}$ depends on $\tilde{\chi} = \frac{\tilde{M}}{\tilde{H}}$, where \tilde{M} is magnetization and \tilde{H} is magnetic field intensity. $\Delta\tilde{\epsilon}$ is the difference of the induced voltage of these two subsidiary coils and $\Delta\tilde{B}$ is the change of magnetic induction. μ_0 is the permeability of vacuum.

By electromagnetic induction law, we can attain that

$$\Delta\tilde{\epsilon} = k_1 \frac{\partial \Delta\tilde{B}}{\partial t}, \Delta\tilde{B} = \mu_0 \tilde{\chi} \tilde{H}, \tilde{H} = k_2 \tilde{I} \quad (8)$$

where k_1, k_2 is the corresponding scale factor with respect to the material and \tilde{I} is the current of voltage-controlled current source OE4201.

By (8) and $\Delta\tilde{\epsilon} = \Delta V e^{i(\omega t + \theta)}$, $\tilde{I} = C V_0 e^{i(\omega t + \theta_I)}$, we get

$$\tilde{\chi} = \frac{\eta}{k_1 k_2 \mu_0} \frac{\Delta V}{C V_0 \omega} e^{i(\theta - \theta_I - \frac{\pi}{2} - \theta_0)} \quad (9)$$

where ΔV represents the amplitude of the difference of the induced voltage, C is the scale factor of the voltage-controlled current source, while V_0 is the input voltage of the voltage-controlled current source. θ and θ_I denote the respective phase associated with the measurements. Additionally, θ_0 accounts for the delay phase introduced by instrument and the eddy current[5].

The parameter η is the loss rate attributed to the eddy current. The difference in phase $\theta - \theta_I - \theta_0$, is referred to as the current delay phase, which is specific to our material and apparatus and should be compensated for during data processing.

Based on equation(9), we can ascertain that the magnetic susceptibility is a complex number, allowing us to extract its imaginary component for analysis.

3.2 Experimental Procedure

In our experiment, precise temperature control ($\Delta T \leq 0.1K$) within a low range (approximately 75 to 95K) and the application of a magnetic field (0 to 2kG) while compensating for the geomagnetic field are crucial.

To achieve accurate temperature control, we utilized a CTI refrigerating machine that is capable of maintaining temperatures around 45K at best. The temperature of the environment was regulated using a PID (Proportional-Integral-Derivative) system. Due to the machine's design, the PT1000 probe used for temperature measurement is not positioned directly at the location of the HTS material, but

rather approximately 5cm away. To obtain real-time temperature readings, we employed a digital multimeter (RIGOL DM3058E) to measure the resistance of another PT1000 sensor placed closer to the HTS material.

In terms of magnetic control, we employed an electromagnetic system capable of generating magnetic fields up to 6kG. However, for safety reasons and to prevent potential damage to the magnetic coils caused by long cooling time (approximately 20 to 30 minutes), we conducted the experiment using magnetic fields below 2kG.

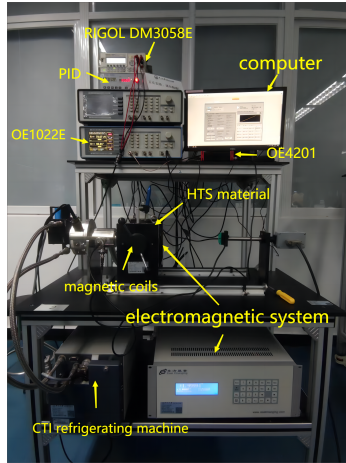


Fig3. All the instruments of our experiment

As mentioned earlier, we utilized a lock-in amplifier (OE1022E) in conjunction with the half bridge method to measure the induced electric field and obtain the AC magnetic susceptibility. Additionally, a voltage-controlled current source (OE4201) was employed to supply a constant current to the primary coils.

To facilitate data analysis and visualization, a computer was utilized. It featured several programs written in LabVIEW language, including a PID control program for temperature regulation, a control and measurement program for the lock-in amplifier, and an electromagnetic system control program. These programs enabled us to display the susceptibility curve in real-time. Should you require access to these programs, we recommend reaching out to our instructor via email.

4 Results and Analysis

4.1 AC Magnetic Susceptibility

In our experiment, the current phase offset $-(\theta - \theta_I - \theta_0)$ was taken by about 33° . More precisely, the current phase offset we chose can be found in Table1.

Magnetic Field B	Geomagnetic		0.0kG	
	cold	heat	cold	heat
$\Delta\phi$	33.00	33.75	32.70	33.45
Magnetic Field B	0.5kG		1.0kG	
	cold	heat	cold	heat
$\Delta\phi$	32.49	33.20	32.35	33.00
Magnetic Field B	1.5kG		2.0kG	
	cold	heat	cold	heat
$\Delta\phi$	32.30	33.00	32.40	33.20

Table1. The current phase offset in each situation

By offsetting the delay phase, we were able to accurately separate the real and imaginary parts of the AC magnetic susceptibility. As a result, we obtained Figure 3, which exhibits a high degree of similarity to Figure 1.

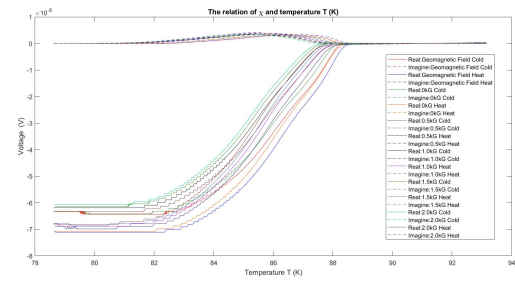


Fig4. AC magnetic susceptibility curve. 'cold' means cooling situation, from high temperature to low temperature; 'heat' means heating situation, from low temperature to high temperature. Solid lines are the real part of AC magnetic susceptibility; Dashed lines are the imaginary part of AC magnetic susceptibility.

In Fig4, through qualitative analysis, we can observe that the critical temperature T_c decreases as the environmental magnetic field increases. Additionally, we observe that the peak temperature of the imaginary part is approximately the midpoint of the decreasing portion of the real part. This alignment between the two aspects indicates the reliability of the results in a qualitative context.

4.2 Critical Temperature T_c

We used the imaginary part of AC magnetic susceptibility to calculate the critical temperature T_c . The resulting critical temperature values are presented in Table 2, and the corresponding curve is depicted in Figure 4.

$B(kG)$	0.0	0.5	1.0	1.5	2.0
$T_{cold}(K)$	85.89	85.61	85.37	85.25	85.13
$T_{heat}(K)$	86.33	85.85	85.66	85.52	85.38

Table2. The influence of magnetic field B on critical temperature T_c .

The absolute slopes of the fitted curve for the cooling situation and heating situation are found to be $k_{cold} = 0.3473K/kG$ and $k_{heat} = 0.3099K/kG$ respectively. Both of these values fall within the possible range of $(0.269, 0.403)K/kG$.

Based on the analysis of Figure 5 and the absolute slope values, it can be suggested that there might be a linear influence of the magnetic field on the critical temperature. This conclusion is supported by the relatively small standard error of $\sigma \approx 0.79K \ll 80K$.

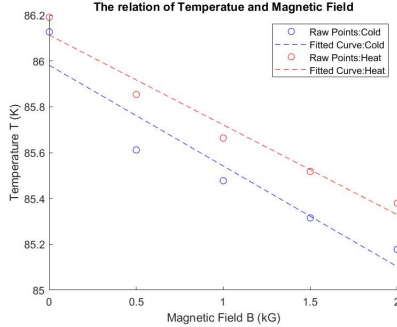


Fig5. Linear influence of magnetic field B on critical temperature T_c . Dashed lines are linearly fitted curves of the relation between B and T_c .

5 Conclusion and Other Possible Explanations

5.1 Other Possible Explanations for the Phenomena

It is well-known that BCS theory is not able to accurately explain the phenomena observed in high-temperature superconductors (HTS) [1]. Therefore, the conclusion drawn from our experiment may not be precise enough. However, there are alternative methods that could be employed to explain the behavior of HTS materials in weak magnetic field environments. These include the Theory of Intrinsic Superconducting States [6], the Soliton model [7], Considering high-energy spin excitations [8], Band structure calculations [9], and the Theory of pair-breaking perturbations [10].

The first method mentioned is a universal approach that can be used to calculate the critical temperature in various situations. It may be worth considering its application in determining the critical temperature under weak magnetic field environments. The second method is specifically tailored for calculating the behavior of HTS material $Y_{1-x}Ca_xBa_2Cu_{2-x}M_xO_{7-\delta}$ and provides a valuable reference point. The remaining three methods have been successfully applied in higher magnetic field environments and to other HTS materials. It is possible to combine these theories with Taylor expansion to obtain more accurate results in our experiment.

5.2 Conclusion of the Experiment

Based on our theory and experimental findings, we have determined the following conclusions: (i) In a weak magnetic field environment ($B \leq 2kG$), the critical temperature T_c exhibits a linear decrease as the magnetic field B increases. (ii) BCS theory provides a rough explanation for the observed

phenomena in HTS material $YBa_2Cu_3O_{7\delta}$ under weak magnetic field conditions.

For future research, it is recommended to conduct additional experiments to obtain more accurate results, as the data obtained in our experiment may be insufficient. Moreover, considering that BCS theory is not fully satisfactory in interpreting the behavior of HTS, it is important to explore other theoretical approaches. In our team's perspective, the theory of pair-breaking perturbations holds promise as a potential explanation for the observed behavior in HTS materials under weak magnetic field environments.

6 Announcement

We have NO commercial purpose in this experiment. The data utilized in our study is derived exclusively from the experiment conducted on March 10th. The original data can be found in the Appendix for reference and further analysis.

7 Thanks

Thanks to SPA for offering us chance and environment to study this experiment. We extend our sincere thanks to our instructor, Mr. Wang, for his invaluable guidance and assistance throughout the experiment. We would also like to acknowledge all the individuals who devoted their time and efforts to contribute to this paper.

8 References

- [1] Orenstein, J., and A. J. Millis. "Advances in the physics of high-temperature superconductivity." *Science* 288.5465 (2000): 468-474.
- [2] Rogachev, A., A. T. Bollinger, and A. Bezryadin. "Influence of high magnetic fields on the superconducting transition of one-dimensional Nb and MoGe nanowires." *Physical review letters* 94.1 (2005): 017004.
- [3] Tinkham, Michael. *Introduction to superconductivity*. Courier Corporation, 2004.
- [4] Ding Shiyong. "AC Magnetic susceptibility Study of Superconductivity." *Progress in Physics* 3 (2009): 239-273.
- [5] Ji Shengmou, Ding Shiyong, and Xu Jianjian. "Influence of AC magnetic field on AC loss of high-temperature superconductors." *Journal of Cryogenic Physics* 29.3 (2007): 233-236.
- [6] Qi Yuefeng. "Theoretical Analysis of Calculating the Superconducting Critical Temperature and Doping of Multicomponent Materials Using the Theory of Intrinsic Superconducting States." MS thesis. Northeastern University, 2010.
- [7] Han Jiahua, and Huang Xiaowu. "Calculate the Transition Temperature of the System $Y_{1-x}Ca_xBa_2Cu_{2-x}M_xO_{7-\delta}$ Using the Soliton Model." *Journal of Anhui University: Natural Science Edition* 20.1 (1996): 25-29.
- [8] Hayden, S. M., et al. "The structure of the high-energy

spin excitations in a high-transition-temperature superconductor." *Nature* 429.6991 (2004): 531-534.

[9] Hunte, F., et al. "Two-band superconductivity in LaFeAsO_{0.89}F_{0.11} at very high magnetic fields." *Nature* 453.7197 (2008): 903-905.

[10] Rogachev, A., A. T. Bollinger, and A. Bezryadin. "Influence of high magnetic fields on the superconducting transition of one-dimensional Nb and MoGe nanowires." *Physical review letters* 94.1 (2005): 017004.

9 Appendix

You can find all the original data here: <https://liuyisi238.github.io/files/OriginalDataOfHTSEExperiment.rar>

You can find the experimental processing code here: <https://liuyisi238.github.io/files/DataProcessingOfHTSEExperiment.rar>

If you want to get the labview program on the computer, please email our instructor: wangk289@mail.sysu.edu.cn

If you want to get more information about this paper and experiment, please email: liuys8@mail2.sysu.edu.cn